Unsteady simulations of Savonius and Icewind turbine blade design using fluid-structure interaction method

Cite as: AIP Conference Proceedings **2187**, 020009 (2019); https://doi.org/10.1063/1.5138264
Published Online: 10 December 2019

Zain Lillahulhaq, and Vivien Suphandani Djanali

Unsteady Simulations of Savonius and Icewind Turbine Blade Design using Fluid-Structure Interaction Method

Zain Lillahulhaq [1, a)] and Vivien Suphandani Djanali [2, b)]

[1]*Mechanical Engineering Department, Institut Teknologi Adhi Tama Surabaya (ITATS), Surabaya, 60111, Indonesia.*
[2]*Mechanical Engineering Department, Institut Teknologi Sepuluh Nopember (ITS), Surabaya, 60111, Indonesia.*

[a)] zain@itats.ac.id
[b)] vivien_s@me.its.ac.id

Abstract. Wind turbine performance can be increased by using the optimum shape of the blade. Most of the previous numerical studies on Savonius wind turbine simulation used constant angular velocity as input data. Usually, the value of constant angular velocity was obtained from experimental data. In the actual case, the rotation of the rotor, i.e. the angular velocity of the blades, results from the interaction between fluids around the wind turbine with the turbine blades, in which there are changes of the moment of inertia. Rotation of the wind turbine can be simulated using the fluid-structure interaction method with one-degree of freedom. This study compares the performance of a rotor turbine using straight Savonius blades, to that using the Icewind turbine blades. In the steady and unsteady simulations, fluid was defined as incompressible, viscous, and uniform air which flow from inlet free stream. The simulation object rotates in one-degree of freedom in the overset mesh area. Icewind turbine generates higher coefficient power compares to the standard Savonius turbine, when it operates at very low wind speed, with the inlet free stream velocity below 4 m/s. This phenomenon is affected by the unsymmetrical shape of Icewind which allowed the fluid flow behind the reversing blade and sweep away the wake area, particularly effective at very low wind speed. The Savonius wind turbine, which is configured with endplates and overlap blades, rotates in high angular velocity and generates the highest peak coefficient of power. Fluid from the advancing blade is flowing through the overlap. The overlap flow fills the wake area and reduces backflow behind the reversing blade.

INTRODUCTION

Human energy consumption rise day by day. In order to decrease fuel consumption, people nowadays attempt to optimizing renewable energy uses. The wind is one of the alternative energy sources, which very popular and harmless to use among the urban area. This paper focuses to study about vertical axis wind turbine (VWAT) especially Savonius model. Savonius is a well-known type of wind turbine since it has many advantages. Savonius wind turbine has a simple construction and easy to maintain. It is suitable to use in the urban area because it can catch wind from any direction. Besides that, a high tower is not needed to support a Savonius wind turbine. Savonius blades can rotate in low wind velocity and be able to self-starting. However, Savonius has lower efficiency compared to the horizontal axis wind turbine (HWAT) Darrieus [1]. Several studies are held to increase the Savonius turbine efficiency. The combination of Savonius and Darrieus wind turbine increases the total efficiency and allows the turbine to self-starting [2]. Furthermore, using a twisted blade, shroud and endplate also raise wind turbine efficiency. Experiments on the optimization of Savonius design including shape, overlap, aspect ratio, and the number of blades, which require gaining wind turbine efficiency. Aspect ratio in wind turbine is the ratio between blade height and rotor diameter. A higher number of aspect ratio indicates an increasing frontal area is affected by the drag force. This extension results in higher efficiency and Coefficient of Power (C_P). A higher number of aspect ratio generates an expanding area affected by backflow. This condition is able to reduce the angular velocity of the wind turbine. The optimum number

Innovative Science and Technology in Mechanical Engineering for Industry 4.0
AIP Conf. Proc. 2187, 020009-1–020009-8; https://doi.org/10.1063/1.5138264
Published by AIP Publishing. 978-0-7354-1934-6/$30.00

of aspect ratio for a Savonius wind turbine is around 0.7 [3]. The number of blades used in the Savonius wind turbine also influences wind turbine efficiency. A higher number of blades indicate more frontal area will be affected by the free stream and backflow. When numerous blades are used in a turbine, more recirculation appears among the blades. A Savonius wind turbine with three blades has the highest efficiency [4]. To reduce the wake region which can resist the turbine rotation, overlap can be added among the blades. There are various blade modifications which can be applied to generate better performance in Savonius wind turbine. Modifications can be performed by twisting or cutting the Savonius blade to create a new form [5, 6].

Icewind turbine is classified as a Savonius turbine type in a new form. It rotates as in the standard Savonius wind turbine blades, which is pushed by the drag force from the free stream. The original idea of the Icewind turbine is reducing the wake area in the returning blade of the Savonius wind turbine. It is designed by cutting the Savonius wind turbine blade and turning it into circular form as shown in Fig. 1. An Icewind turbine is able to rotate in a low free stream velocity. In high free stream speed operation, Icewind turbine will have peak of efficiency in a lower rotating speed. This condition prevents the over speed problem in wind turbine which is often caused by extreme weather, lubricant failure, or vibration.

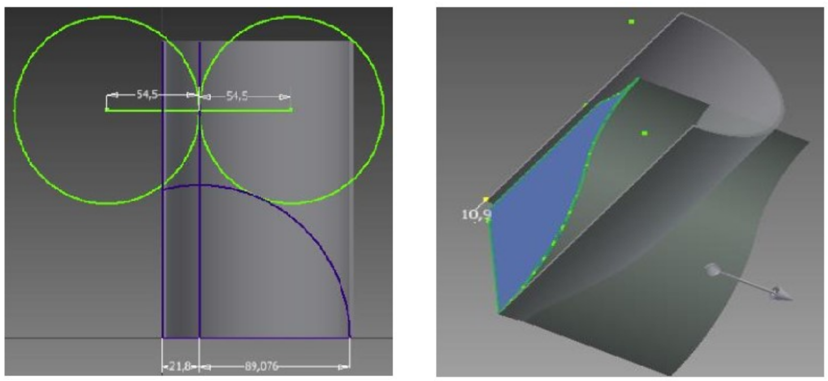

(a) (b)

FIGURE 1. Icewind turbine drawing process (a) sketch cutting area (b) trim sketch on blade

The study of Savonius wind turbine performance can be performed using numerical simulations to get qualitative and quantitative data. The simulations can be performed in two-dimension or three-dimension, in steady or unsteady condition. Commonly, numerical studies are processed using a constant angular velocity as an input and initial condition to have a result as a function of Tip Speed Ratio (TSR). Otherwise, using load to get a TSR function in a constant angular velocity causes fluctuation in turbine output data [7]. Constant angular velocity input data give an assumption that there are loading or brake system in the Savonius axis. Loading condition in the numerical study may give different result compared to that in simulation without loading at the same TSR [8]. Moreover, the use of constant angular velocity cannot be used to optimize a new form of a wind turbine, in which there is no experimental data on the angular velocity available yet.

In this study, angular velocity is the output of the numerical study and not used as input data. The value of the angular velocity is obtained from the interaction between the free stream and Savonius blades. To solve this case, the Fluid-Structure Interaction (FSI) method can be applied to simulate the rotating blades. FSI is a numerical method which solves the interaction between a structure and the fluid around it. This method can detect any force and movement of the structure. Discretization of the FSI method depends on both the fluid characteristic and the cross-section area. FSI method does not require the value of the angular velocity as an input, but it requires the mass and moment inertia of the structure. The FSI method is suitable to be used to solve the case of optimizing new form of a wind turbine such as an Icewind turbine, in which the available data is dimension and mass. This paper discusses Savonius and Icewind turbine characteristics using FSI method. The characteristics can be observed from the qualitative data such as C_P and C_Q, and quantitative data such as velocity vectors and pressure contours.

NUMERICAL METHOD

Vertical axis wind turbines with three blades are simulated in steady and unsteady condition by using Finite Volume Method. The simulations use two blade variations, which is the standard Savonius blade and the Icewind blade as shown in Fig. 2. The first configuration was the standard Savonius blades, without endplate and no-overlap. This turbine has a shaft to connect the blades. The second configuration was the standard Savonius blades, equipped with endplate and overlap. The rotor turbines, which are used in this simulation, have the same number of blades, frontal area and density. The rotor dimension was similar to the experiment of [6], but with three blades used in this study, as shown in Table 1. The third configuration was the Icewind turbine, which formed from Savonius blades with dimension in table 1. This blade is cut into a new shape of turbine, shown in Fig.1, and rotated the blades in a shaft. Then it enlarges until it has same frontal area with Savonius wind turbine. The icewind turbine has the aspect ratio (D/H) 1.33. The turbines in this simulation have same wide of frontal area.

The grid used in this study has been obtained from a grid independency test, as documented in [9]. The simulations were run in Reynolds Averaged Navier Stokes (RANS) in k-ω STT turbulence model. The parameters and boundaries used in this simulation is shown in Table 2. The moment of inertia and mass of the rotor wind turbines were used as an input data, and obtained from the dimension, shape and material of the rotor. This data is crucial as an initial condition in FSI simulation. The maximum value of CFL number for stability and convergence solution of dynamic simulation and implicit Euler integration is 5, as in [10], and this value is considered to calculate the time step of the unsteady simulation.

Table 1. Dimensions of the Savonius wind turbine

Name	Value
Overlap (e / d)	0.15
Aspect ratio (D/ H)	1.58
End plate (D / d)	1.1
Number of blades	3

Table 2. Parameters used in the numerical simulation

Parameters	Input	Value
Fluid properties	Density	1.225 kg/m^3
	Absolute viscosity	1.86 x 10^{-5} $N.s/m^2$
Inlet boundary	Velocity inlet	2 - 10 m/s
	Turbulence intensity	4%
	Length scale	0.01 m
Outlet boundary	Pressure outlet	0 Pa
Rotor blades	Rotating axis	y-axis
	Material	Galvanized Iron
	Density	7870 kg/m^3
	Massa	3.1305 kg
	Moment of inertia	0.017175 $kg.m^2$
Solver	Maximum residual	10^{-4}
	Spatial discretization (momentum)	Second order upwind
	Pressure discretization	Second order
Unsteady solver	Time discretization	Implicit second order
	Time step	Based on CFL < 5
	Inner iteration	100 iteration /time step
Tubulence model	RANS Segregated flow k-ω SST	

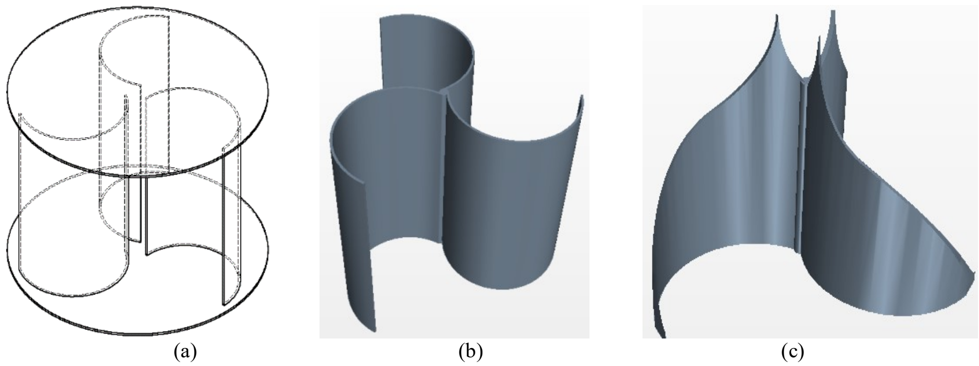

FIGURE 2. (a) Savonius wind turbine with overlap and endplate (b) Savonius wind turbine without endplate and without overlap (c) Icewind turbine.

In the FSI 1-DOF method, there is a static region which is stated as the test section. Another section is the rotating region, i.e. the moving mesh, which is stated as the overset area, such as that shown in Fig. 3. The overset mesh is set in the area of the rotor to create the rotating effect. In the mesh, uniform trimmer surface remesher model is used, as shown in Fig. 4. To get the y^+ value close to 1, the mesh used prism layer option, with 10 layers, around the blade surface. The total number of 1,100,000 cells were used the simulation to obtain a stable result. The FSI 1-DOF method is calculating the simulation in unsteady condition within a designated number of time steps. The simulation run from the idle condition up until the rotor turbine reaches steady angular rotations. In the FSI 1-DOF method, the optimum value of C_P and C_Q are taken from average value of certain interval time. Meanwhile, the static simulations were run steady in different azimuth angles. The azimuth angle (Θ) was using a reference of 0° in the horizontal direction upstream of the rotor, parallel to the free stream direction, and the angle Θ is counted in clockwise direction, as shown in Fig. 5. The average C_P and C_Q values in various azimuth angles are considered as the total C_P and C_Q value from a rotating turbine.

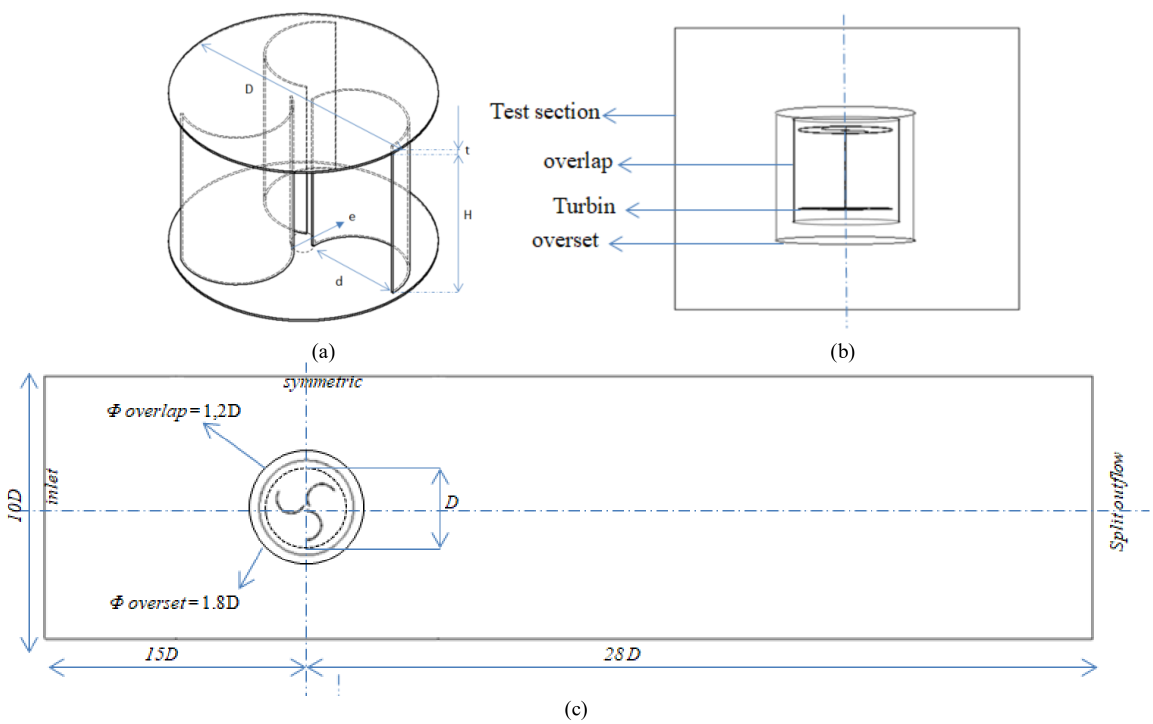

FIGURE 3. (a) Savonius wind turbine and Boundary condition and size of test section (b) side view (c) top view.

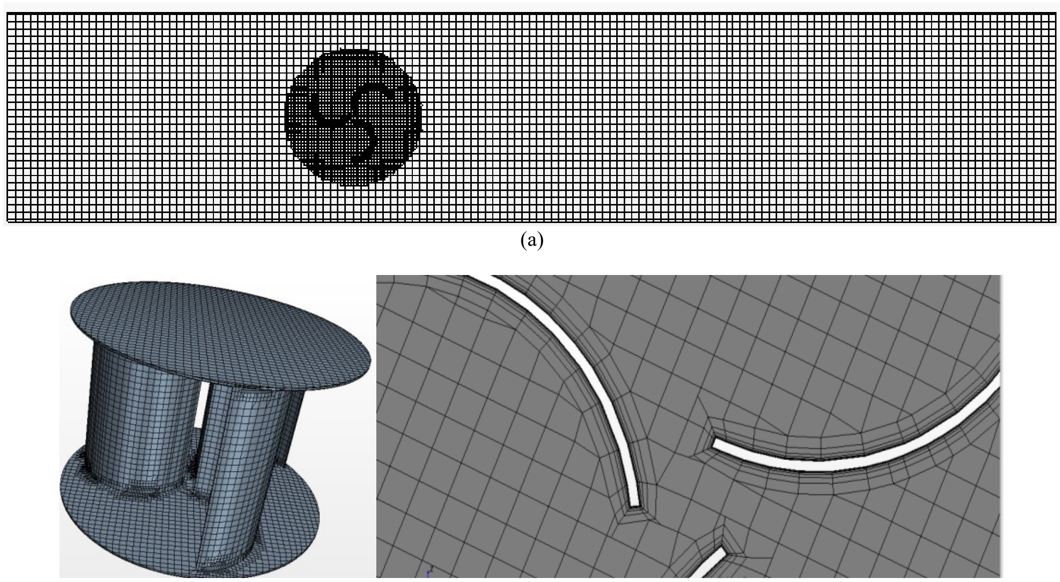

(a)

b) (c)

FIGURE 4. Detail mesh view on (a) Test section and overlap (b) Savonius wind turbine with endplate and overlap (c) layer mesh near surface blade.

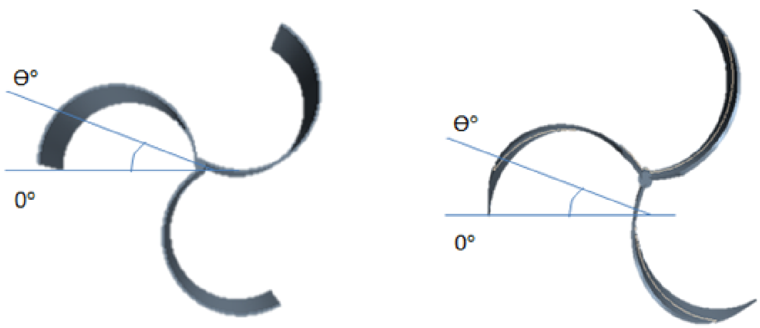

(a) (b)

FIGURE 5. Azimuth angle on (a) Savonius wind (b) Icewind turbine.

PERFORMANCE CALCULATIONS

Several parameters are derived from the simulation results, such as Tip speed ratio (TSR), Coefficient of power (C_P), and Coefficient of torque (C_Q) to express the wind turbine performance. The TSR is a non-dimensional number to describe velocity. The torque and power generated by the wind turbine are stated as non-dimensional parameters of C_Q and C_P, respectively. The equations are shown as follows:

$$TSR = \frac{\omega.d}{v} \tag{1}$$

$$C_P = \frac{T.\omega}{\frac{1}{2}\rho.D.H.v^3} \tag{2}$$

$$C_Q = \frac{T_{actual}}{\frac{1}{4}\rho.A_S.d.v^2} \tag{3}$$

with, TSR	: Tip speed ratio	C_P	: Pressure coefficient
ω	: Angular velocity (rad/s)	C_Q	: Torque coefficient
d	: Blade diameter (m)	H	: Wind turbine height (m)
v	: Freestream velocity (m/s)	D	: Wind turbine diameter (m)
T	: Torque of wind turbine (Nm)	A_s	: Frontal area (m^2)
ρ	: Density(kg/m^3)		

RESULTS

Unsteady simulations of the three-dimensional turbine rotors were run in varying freestream velocity of 2 m/s to 10 m/s. Figure 6 shows the coefficient of torque graphs as a function of freestream velocity. The result shows that, in general, the value of C_Q is increasing along with increasing freestream velocity. The standard Savonius wind turbine without overlap and endplate results the lowest C_Q value. Meanwhile, the Savonius wind turbine equipped with endplate and overlap resulted the highest C_Q when it operates in the freestream velocity above 4 m/s. The Icewind turbine results the highest C_Q in a low freestream speed, i.e. when the velocity is below 4 m/s. When the Icewind turbine is operated in a higher free stream velocity, it results a lower torque coefficient than the standard Savonius turbine with overlap and endplate. This suggests that the Icewind turbine is suitable to be installed in low wind speed area.

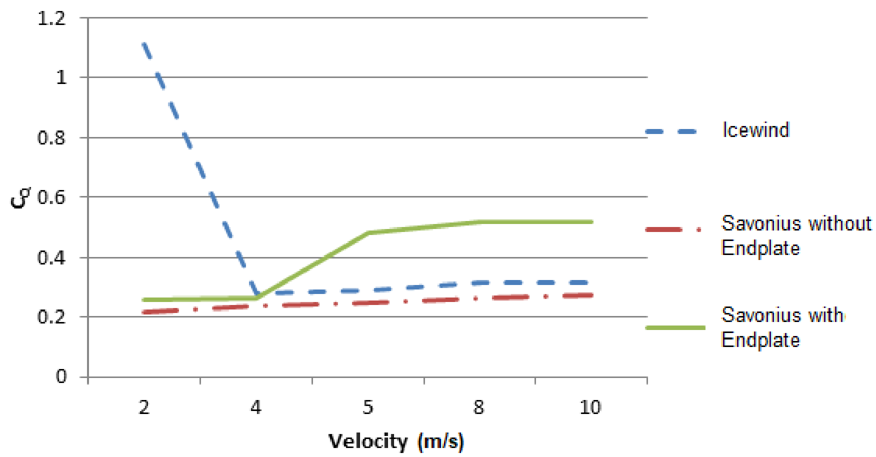

FIGURE 6. The coefficient of torque as a function of velocity for various types of wind turbines

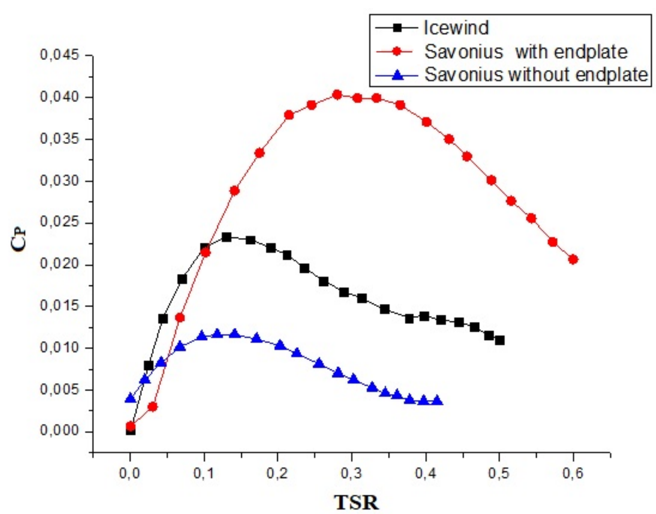

FIGURE 7. The coefficient of power as a function of tip-speed ratio for various types of wind turbines.

The difference of characteristics between the three rotor configurations is shown in Fig. 7. The Savonius with endplate and overlap has the highest peak C_P value compared to that of the other turbine variations. It is shown that the Savonius wind turbine equipped with overlap and endplate generates the highest power, with wider range of TSR. Meanwhile, the Icewind turbine results in higher C_P value when TSR is below 0.1. This implies that the Icewind turbine has better performance in low speed operations. The Savonius turbine without overlap and endplate has the lowest C_P value. However, the Savonius turbine without overlap and endplate results higher C_P value in a very low TSR.

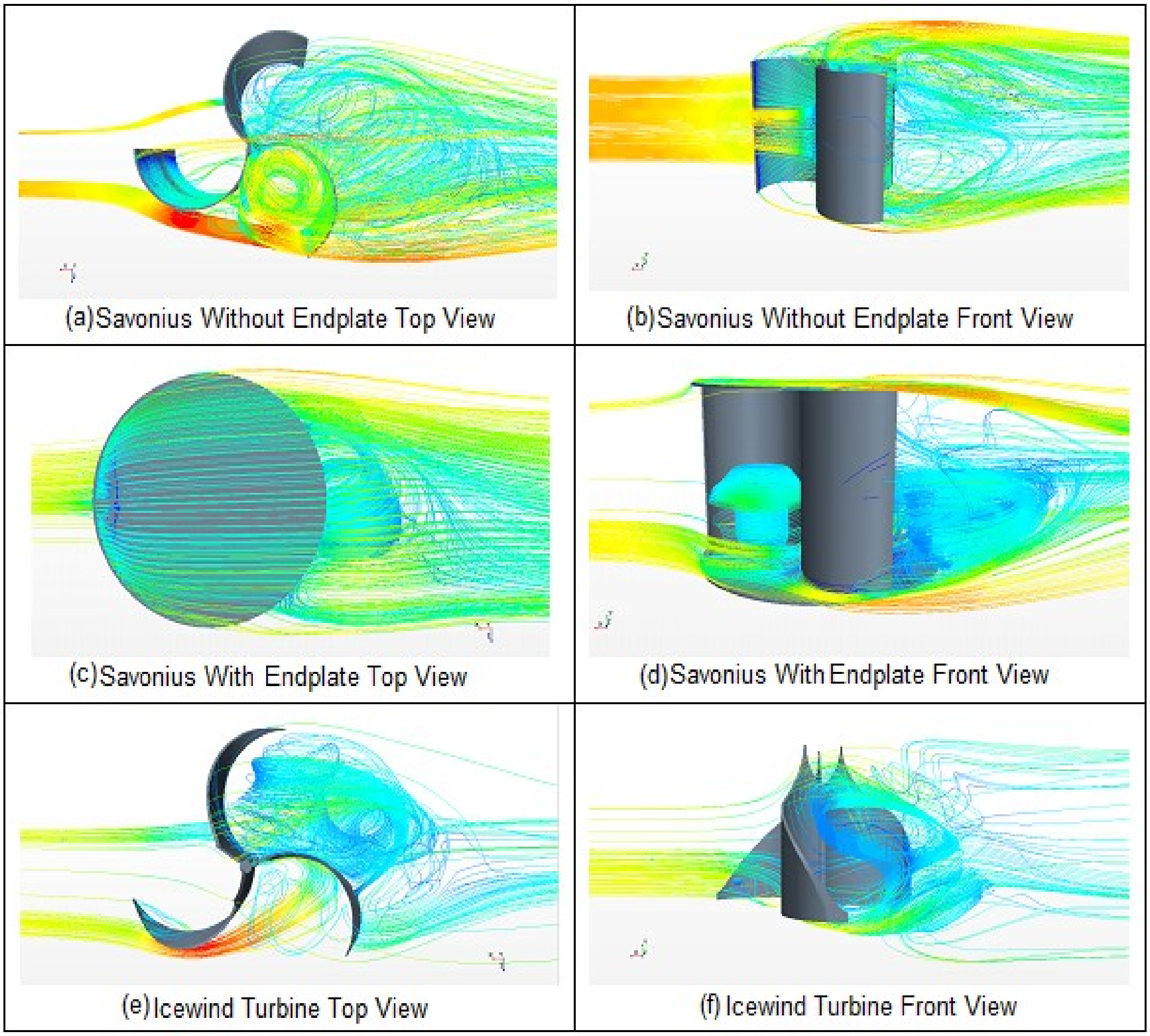

FIGURE 8. Pathlines of the flow around the rotor turbine (a,b) Savonius wind turbine without endplate and without overlap, (c,d) Savonius wind turbine with endplate and overlap, and (e,f) Icewind turbine

The path lines of the flow around the rotor blades at a position of 0º azimuth angle at a velocity of 5 m/s are shown in Fig. 8. In Savonius rotor without end plate and overlap, the flow generates wide wake area behind the turbine blades. This wake area is similar to that occurs on the vertical cylinder. When the fluid hit the frontal area of the blades, it generates vortices in front of the blades. These vortices prevent the freestream flowing through blade surface and separate the flow into three directions. The flow which passes through the blade tip, forms wake area behind the blades. The fluid also flows on the top and bottom of the blades, exaggerating the vortex formation behind the blades. This vortex is whirring around and reducing the rotor rotational speed. Meanwhile, the freestream that flows at a certain distance from the blade side has no interaction with the blade surface. The Savonius blades equipped with endplate and overlap has only slight vortices compared to that on the Savonius blades without endplate and overlap.

The overlap gap between the Savonius blades is able to avoid wake formation in the upstream area. The freestream fluid is able to pass over the surface of the blade and flow through the gap. This jet flow fills the empty area behind the blades and flushes the vortices behind wind turbine. This reduces the wake area. The endplates at the bottom and top of the blades avoids the freestream from flowing into the empty area behind the blades. The Icewind turbine has different shape to the Savonius blade. The peripheral of the Icewind turbine varies as a function of the rotor height. The curvature surface of the Icewind turbine results in a smaller wake area.

SUMMARY

In this study, three-dimensional simulations of the Savonius and Icewind rotor turbine were performed by using the unsteady FSI 1-DOF method. Several conclusions from the study are:

- The Savonius wind turbine which equipped with endplate and overlap resulted in the highest coefficient of power compared to the other configurations. For Savonius blades with overlap and endplates, the gap between blades results on flushing effect which can reduce the wake area. Moreover, the use of endplates at the top and bottom of the blades helps reducing vortice formation behind the blades.
- The Icewind turbine generally has better performance compared to the Savonius turbine without endplate and overlap. Moreover, in tip-speed ratio lower than 0.1, the Icewind turbine has the highest C_P value which implies that the Icewind turbine has the best performance for a very low wind speed operation.

REFERENCES

1. T. Letcher, The Ohio State University, Columbus,OH, 2010.
2. X. Liang, S. Fu, B. Ou, C. Wu, C.Y. Chao, K. Pi, Renew Energy Vol. 113, pp. 329-334 2017.
3. M. Kamoji, S. Kedare, S. Prabhu, International Journal of Energy Research32 (10), pp. 877-895, 2008.
4. M.H. Ali, International Journal of Modern Engineering Research (IJMER), Vol. 3, Issue. 5, Sep - Oct. 2013 pp-2978-2986, ISSN: 2249-6645, 2013.
5. M. Tanhani, A.Rabbani, A. Kasaeian, M. Mehrpooya, M. Mirhosseini, 10.1016/j.energy.2017.04.125, 2017.
6. S. Roy, UK. Saha, Appl Energy 2015;137:117–25, 2015.
7. T. Wakui and R. Yokoyama, , Wind Engineering, 31(1), 43–58, 2007.
8. A. Al-Faruk and A. Sharifian, Energy Procedia 110 (2017) 235 – 242, 2016.
9. Z Lillahulhaq and V.S. Djanali, IPTEK Journal pp 48 – 52, ISSN: 2354 - 6026, 2019.
10. P. Jaohindy, H. Ennamiri, F. Garde, A. Bastide, Wind Energy, Wiley, 2014, 17 (6), pp.853-868, 2017.